EUROPEAN ORGANIZATION FOR NUCLEAR RESEARCH
ORGANISATION EUROPEENNE POUR LA RECHERCHE NUCLEAIRE

CERN - PS DIVISION

PS/ RF/ Note 98-04

RF MEASUREMENTS AND TUNING OF THE ACCELERATING SECTION HCS2

R. Bossart, M. Chanudet, CERN, Geneva, Switzerland
G. Bienvenu, LAL, Orsay, France

Geneva, Switzerland
4 March 1998

RF MEASUREMENTS AND TUNING OF THE ACCELERATING SECTION HCS2

1. Introduction

The accelerating section HCS2 was tuned and measured at CERN from 16.12.97 to 18.12.97 and from 06.01.98 to 14.01.98. The delicate operations were done in collaboration with G. Bienvenu (visiting CERN from 06.01.98 to 09.01.98).
Section HCS2 was tuned after the machining of the tuning holes, the mounting of the screws for cell deformation and the brazing of the water cooling pipes.
The successive steps of tuning HCS2 are resumed. The CW and pulse measurements on the final state of the structure are reported hereafter.

2. Matching of the section

In CTF, section HCS2 must operate with travelling waves in the mode $11\pi/12$. Its nominal frequency is 2990.740 MHz in vacuum at 30°C or 2990.240 MHz under atmosphere in normalised conditions (20°C, 760 Torr, 60% of humidity).
At the beginning of the tuning, the different cells oscillated 800 kHz below the nominal frequency with a maximum dispersion of ±100 kHz. The two couplers were identical, the dimensions of their coupling apertures and their frequency were adjusted at LAL before the brazing of the section.
The operation began with the tuning of the 13 cells. The frequency of all cells was increased by the same value to reach an average phase shift per cell of about 165° ± 2°. Then, the frequency of each cell was individually changed to smooth the electrical field in the section. In particular, it is useful to view the transmission of the section when a little ceramic is moved on the axis of the section. The uniformity and the minimisation of the transmission loss allow to optimise each cell with good sensitivity. Then, tuning input and output couplers decreases the mismatches inside the section. At the end, the input coupler allows to minimise the SWR (Standing Wave Ratio) at the entrance of the section. It is necessary to repeat these steps several times to obtain a good matching of the section.

3. Status of HCS2

In the following sections, the status of the main low power RF characteristics of the accelerating section HCS2 is reported after its final tuning.

3.1 Electric field on the axis

With a small cylindrical ceramic bead (C) of dimensions ∅ 1 × 6 mm moved along the axis of the section, the amplitude and phase of the electric field were plotted (see figures 1 and 2).

3.1.1 Magnitude

At nominal frequency, the maximums of the electric field in each cell are relatively uniform. They vary less than 18% in voltage (or 1.5 dB in power) around the average value. There is no under-voltage in the last cells of HCS2 as it occurs in HCS1.
In the two couplers, an over-voltage 17% higher than the normal value is measured. We can notice that the field of the input coupler is the highest one of the section. With high power, RF break down will be most probable there.
From the input to the output, the RF power is attenuated by –4.0 dB, so 40% of the incident power is transmitted to the output load.

3.1.2 Phase shift per cell

The measurement of the phase shift involves the forward and backward waves, thus the measured phase is equal to 360° -2×φ as shown in figure 2. The average phase shift per cell is -163.5°, i.e. 1.5° smaller than the nominal value of 165°.The phase shift is really regular except for the first 3 cells where it is less than -159°. Another measurement of the phase by the mean of a short-circuit (SC) moved along the axis gives similar data at ±3° (see table 1).

	1	**2**	**3**	**4**	**5**	**6**	**7**	**8**	**9**	**10**	**11**	**12**	**13**	**14**
C	36°	43°	46°	42°	34°	28°	27°	28°	28°	28°	30°	32°	34°	31°
SC	39°	46°	46°	40°	32°	27°	25°	28°	30°	32°	34°	34°	34°	30°

Table 1: Phase measured with a small ceramic (C) or a short-circuit (SC)

3.1.3 Acceleration

Thanks to the amplitude and phase measurement of the electrical field along the axis, the acceleration of an electron in phase with mode 11π/12 can be calculated. Figure 3 gives the expected experimental acceleration voltage in function of the phase of the electron at its arrival in the input coupler. This acceleration voltage is normalised to the value corresponding to a theoretical electric field with 15% of over-voltage in the couplers. Then, the acceleration amounts to 94% with a particle phase of 0° and reaches 99% with a particle phase of -18°.

3.2 Reflection coefficient at the input

The reflection coefficient at the input of HCS2 is shown in figure 4. Over the passband, there are 13 resonant frequencies for 15 cavities; the modes 0 and π do not appear because their losses are too high (extremities of the passband).
Near the nominal frequency, the reflection coefficient is given by figures 5 and 6 in logarithmic and polar co-ordinates respectively. The 11π/12 mode is well adapted to the RF source. The reflection coefficient passes round the centre ρ = 0 with reflection below -25 dB over 300 kHz. The SWR of the nominal frequency reach -31 dB (less than 10^{-3} of power is reflected).

3.3 Transmission and delay

The width of the passband of HCS2 is 27 MHz. The 13 resonant modes also appear on the transmission measurement with small bumps of the S21 coefficient (see figure 7). The nominal frequency is just below the last peak of the passband as the 11π/12 mode is only 450 kHz below the mode π. For the 11π/12 frequency, more than 40% (or -3.8 dB) of the incident power is transmitted to the output (compared to the -4.0 dB found with the measured electric field).

Moreover, the phase delay between input and output couplers is shown in figure 8 as a function of the frequency. The nominal mode travels trough the section in about 640 ns. But this time varies quickly for a small frequency shift. For example, 400 kHz further, the phase delay reaches its maximum of 870 ns.

3.4 Adaptation of the couplers

To obtain information about the adaptation of the two couplers separately, the method of Gallagher [1] was used with two movable short-circuits on the output waveguides. The measured Smith chart is plotted in figure 9. The reflection coefficient of the input and output couplers are represented by the S (Smith) and I (Iconocentre) points respectively. Each coupler seems well adapted with reflections below 4%. According.to the RLC analysis of the section, the frequency of the output coupler is a little smaller than for the input (points go counter clockwise).
The attenuation of the section can also be calculated and gives once more -4.0 dB.

4. Pulse response of HCS2

The pulse response of a TW structure is limited by the frequency bandwidth of the passband. For operation with a phase advance of $11\pi/12$ close to the π-mode, a large amount of the pulse power spectrum is situated at frequencies above the passband ending with the π-mode (Fig. 7).The input power outside the bandwidth of the TW structure is reflected back to the power source at the beginning and at the end of the RF pulse, as it is well known from SW structures. The group velocity of the travelling wave decreases towards the π-mode and the filling time of the structure increases accordingly.

There is a strong modulation of the phase delay due to the 13 resonance peaks of the passband (Fig. 8). The steeper the slope of the phase delay, the more it becomes difficult to match the impedance among the individual cells and couplers. Small mechanical errors during the machining of the cells or slight mechanical deformations of the structure during the brazing of the cells or water pipes do cause large cell mismatches of the group velocity, proportionally to the slope of the phase delay. As illustrated in figure 8, the mode $11\pi/12$ is sitting exactly at the frequency shown by marker 1, where the slope of the phase delay is steepest in the entire passband. It is therefore not astonishing that it was so difficult to tune the structure for correct operation. The mode $\alpha\pi$ shown by marker 4 in figure 8 would have been much easier to tune for TW-operation! Fortunately, the deformation holes of each individual cell could be equipped with ingenious push-pull screws [2] so that the cell walls could be deformed inwards and outwards for a reversible tuning of the cell's frequency.

4.1 Transient Reflections of HCS2

The rise and fall time of the RF power pulse generated by the klystron is 100 ns typically. For such a short rise and fall time of 100 ns, the input coupler of HCS2 reflects 16% of the incident power, i.e. 40% of the incident voltage. Although the reflected power decays rapidly with an e-folding time of about 150 ns, the voltage reflected at the beginning of the pulse may deflect the electron beam of the klystron. However, the reflected power r^2 at the pulse start reduces drastically for a slower rise time 0.5 µs.

$t_r = t_f$	r^2 (start)	r^2 (stop)
0.1 µs	0.16	0.14
0.2 µs	0.08	0.14
0.5 µs	0.03	0.07

Table 2 : Reflected power r^2 as a function of the rise and fall time t_r and t_f. PW = 3 µs

The transient reflections at the start and stop of the RF pulse reveal a double peak culminating at 0.2 µs and 0.8 µs after the start of the power rise and fall (see photos 1-2). The fast peak is caused by the coupler which has a larger frequency bandwidth than the cells.

4.2 Fill time of HCS2

The fill time of the HCS2 structure has been measured between the input (photo 1) and output coupler (photo 3). The fill time τ for pulsed operation is the sum of the propagation delay t_{pd} of the RF power from the input to the output coupler and of the rise time at the output : $\tau = t_{pd} + t_{r2}$.

The propagation delay is measured between the start of the RF pulse at the input coupler and the time when the output power reaches 10% of the final value : t_{pd} (0-10%) = 0.65 µs. The

propagation delay of HCS2 agrees rather well with the phase delay 0.64 μs measured by the network analyser for CW excitation.
The rise time of the output power is limited by the frequency bandwidth Δf between the modes 11π/12 and π: Δf = 450 kHz. Theoretically, the rise time t_{r2} (10-90%) for a Gaussian filter chain, representing rather well the HCS structure, is given by [3] $\mathbf{t_{r2} \cong 0.35/\Delta f = 0.75\ \mu s}$.

The fill time of HCS2 has been measured for different power levels 80 - 90 - 100% of the final output power and for different RF frequencies, see table 3.

Frequency (f_o = 2990.2 MHz)	Fill Time for Output Power Level 80%	90%	100%
f_o + 100 kHz	1.4 μs	1.7 μs	2.0 μs
f_o (11π/12)	1.1 μs	1.3 μs	1.5 μs
f_o - 100 kHz	1.0 μs	1.1 μs	1.2 μs
f_o - 1 MHz (5π/6)	0.4 μs	0.45 μs	0.5 μs

Table 3 : Fill time τ versus frequency for different output power levels 80-90-100%

The accelerating voltage in the HCS structure reaches its final value after 1.5 μs for the nominal accelerating frequency f_o. This is twice as long as the phase delay of 0.7 μs assumed as fill time by the design study of CTF2.
In order to gain more peak power from the LIPS pulse compression, the pulse length of the HCS power input can be reduced to 1.3 μs.
However, the higher peak power will induce RF breakdowns more frequently, and the beam will be affected by the parasite modes of the HCS structure during the fill time.

The fill time of the HCS structure is much shorter if the frequency separation from the π-mode increases. For the mode 5π/6 just 1 MHz below the nominal frequency f_o, the fill time amounts to 0.5 μs. This mode can be used for power tests of the accelerating section. For beam acceleration by the mode 5π/6, the accelerating voltage of the HCS drops to 60% of the nominal mode 11π/12.

4.3 Overvoltage of the Input Coupler

It is known from other TW accelerating structures that the accelerating field is considerably higher in the couplers than in the neighbour cells. The accelerating field measured by bead pulling through HCS2 is 50% higher in the input coupler than the average field of the structure : $E_{in}/E_{eff} = 1.5$.
It is therefore most likely that the RF breakdowns happen in the input coupler. Field simulations by MAFIA or HFSS should be carried out to study the field configuration on the copper surface, especially at the beam irises of the coupler where field breakdowns are expected.
The transient response of the input coupler has been measured for an RF pulse by a field probe placed on the beam axis in the beam pipe of the input coupler. Photo 4 shows the pulse overshoot of 26% peak power at 0.8 μs after the start of the RF pulse. The transient overvoltage in the input coupler amounts to 13% peak amplitude and lasts for 0.8 μs. It is known that voltage overshoots of 10% on the copper surface increase the dark current by about 50% [4], and that these transient voltage overshoots and electron emissions of the input coupler trigger the RF breakdowns of the HCS structure.

It has been calculated by an RF field simulation programme for different modes of HCS that the ratio between the surface field E_s on the iris and the average accelerating field E_{eff} on the beam axis is a minimum for the mode $11\pi/12$: $E_s/E_{eff} = 2.39$ [5]. For the π-mode, only 450 kHz higher, the surface field of the regular cells is larger: $E_s/E_{eff} = 2.96$.
No simulations have been made for the coupler cells, which clearly have a breakdown problem. Adding the evanescent fields of the power transportation from the coupling hole of the waveguide to the neighbour cell, it can be estimated that the field on the copper walls of the coupler cells is $E_s/E_{in} > 3$.

4.4 High power operation and RF breakdowns

For nominal operation the HCS structure shall be powered by 120 MW and should impart to the beam an unloaded energy gain of 38 MeV on crest of the RF-wave [6]. The average field gradient of the HCS structures is E_{eff} = 60 MeV/m for nominal operation, or E_s = 145 MV/m on the copper surface of the cells.
At the input coupler, the peak accelerating field is 170% (1.5x1.13) of the average field : E_{in} = 100 MeV/m. On the irises of the coupler, the surface field would rise to $E_{si} > 250$ MV/m. Such high fields have never been reached for S-band structures pulsed during 1 μs. It will be no surprise if the HCS structures have breakdown problems well below the enormous input power of 120 MW.
Nevertheless, any endeavour must be undertaken to improve the surface cleanliness of the high gradient structures and the waveguiding system [7]. The vacuum system of CTF2 must be improved to an ultrahigh vacuum pressure of 10^{-9} ... 10^{-10} Torr in the HCS structures.

5. Conclusion

The accelerating section HCS2 is better matched than HCS1. Some of their RF characteristics are compared in the following table.

	Fo (MHz)	SWR (dB)	Δf SWR (kHz)	Del. (ns)	Att. (dB)	<φ>	Acc.	Refl. Cin	Refl. Cout
HCS1	3006.360	-31dB	100*	820	-5.2	-165.5°	91%	6%	25%
HCS2	2990.740	-31dB	300	640	-4.0	-163.5°	94%	4%	4%

Table 4 : HCS1 and HCS2 RF characteristics

Δf SWR means frequency bandwidth for SWR below -25dB.
* Reflection coefficient with "T" correction.

6. Acknowledgements

We gratefully acknowledge the help of J.C. Godot and A. Ruck for the modification and adjustment of the reversible deformation holes and for the cell tuning.

References

[1] W. J. Gallagher, "Measurement Techniques for Periodic Structures", Microwave Laboratory, Standford California, M.L. report no 767, November 1960.

[2] J.C. Godot, A. Ruck, "Test en Préparation de la Correction de l'Accord de la Section HCS1", memorandum 1.10.1997 (PS/LP).

[3] H.J. Blinchikoff and A.I. Zverev, "Filtering in the Time and Frequency Domains", New York 1976, p. 141.

[4] R. Bossart, "Beam Loading of RF Gun by Dark Current", CLIC Note 138, 1991.

[5] G. Bienvenu, Private Communication.

[6] G. Bienvenu and J. Gao, "A high Current High Gradient Electron Double Accelerating Structure", Europ. Part. Acc. Conf. Barcelona, 1996, p. 495.

[7] R. Bossart, "Synthèse des Procédures de Dégraissage, de Nettoyage et d'Etuvage des Canons RF des Structures HCS et des Guides d'Onde CTF", PS/RF/Note 98-03.

Pulse Response of HCS2

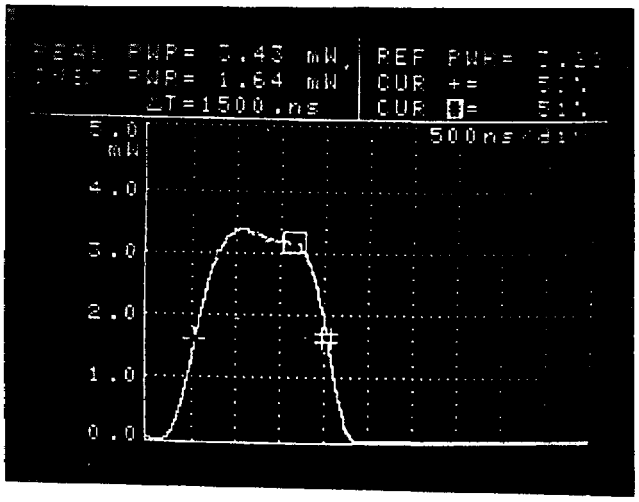

Photo 1 : Incident Input Power
t_r = 0.5 μs, PW= 1.5 μs fwhm

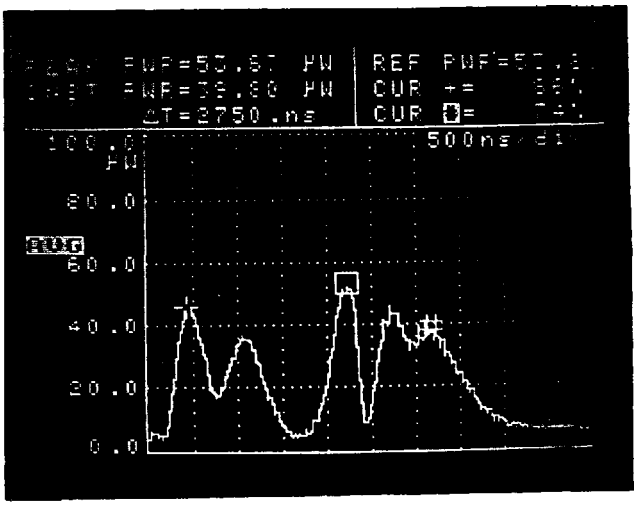

Photo 2 : Reflected Input Power
r = 1.6·53 μW/3.4 mW = 2.5%

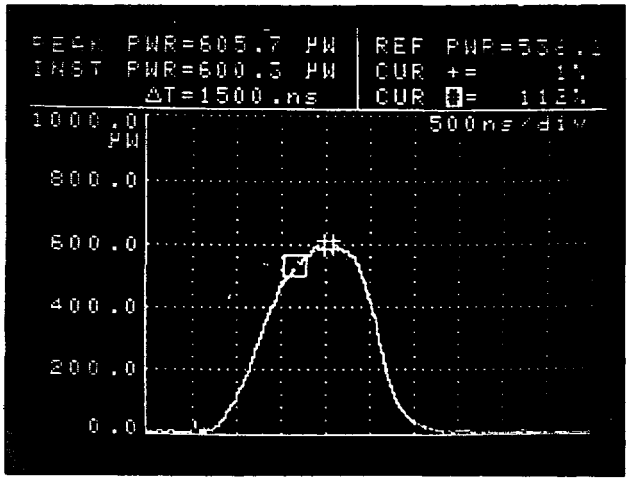

Photo 3 : Output Coupler Power
t_{pd} = 650 ns, t_{r2} = 750 ns, τ = 1.4 μs

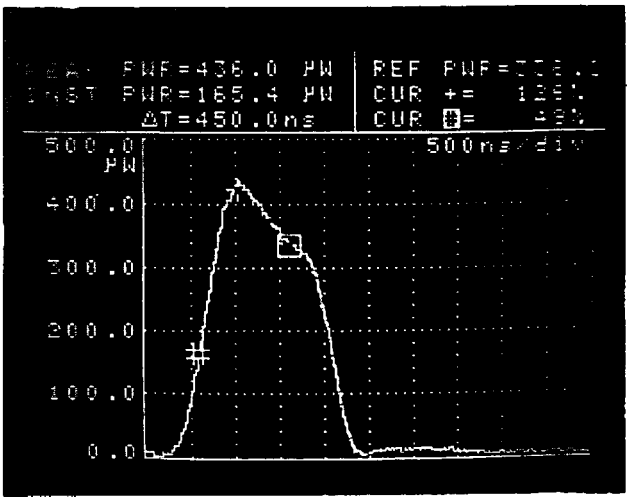

Photo 4 : Field Probe of Input Coupler
Transient Power Peak : 126%

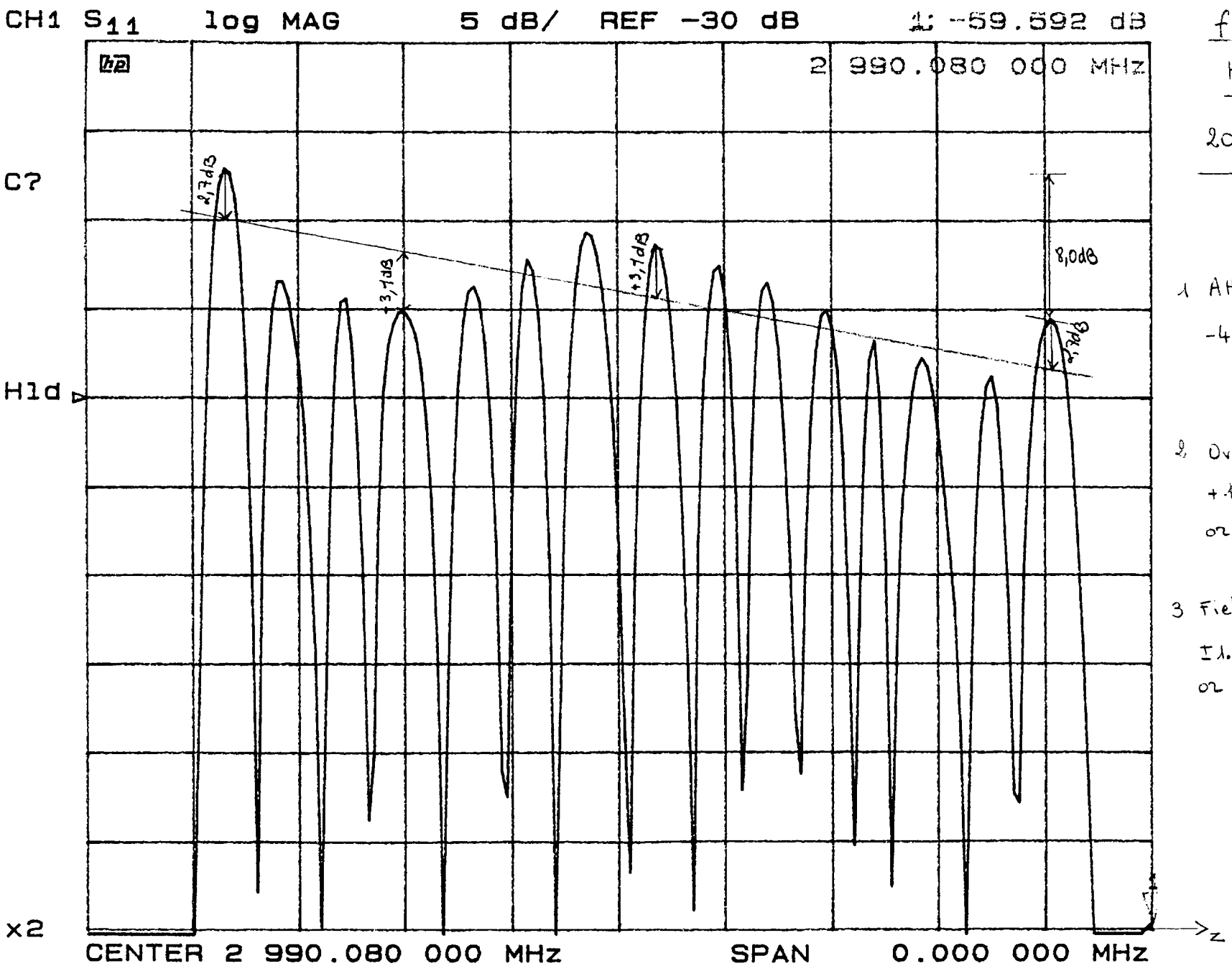

figure 1:

HCS2

$20 \log_{10} E^2$

1 Attenuation
−4.0 dB in power

2 Over-voltages in couplers
+1.35 dB in power
or $1.17 E_0$

3 Field variations
±1.5 dB in power
or ±18% E_0

T = 21.4 °C
P = 755 Torr
H = 52%

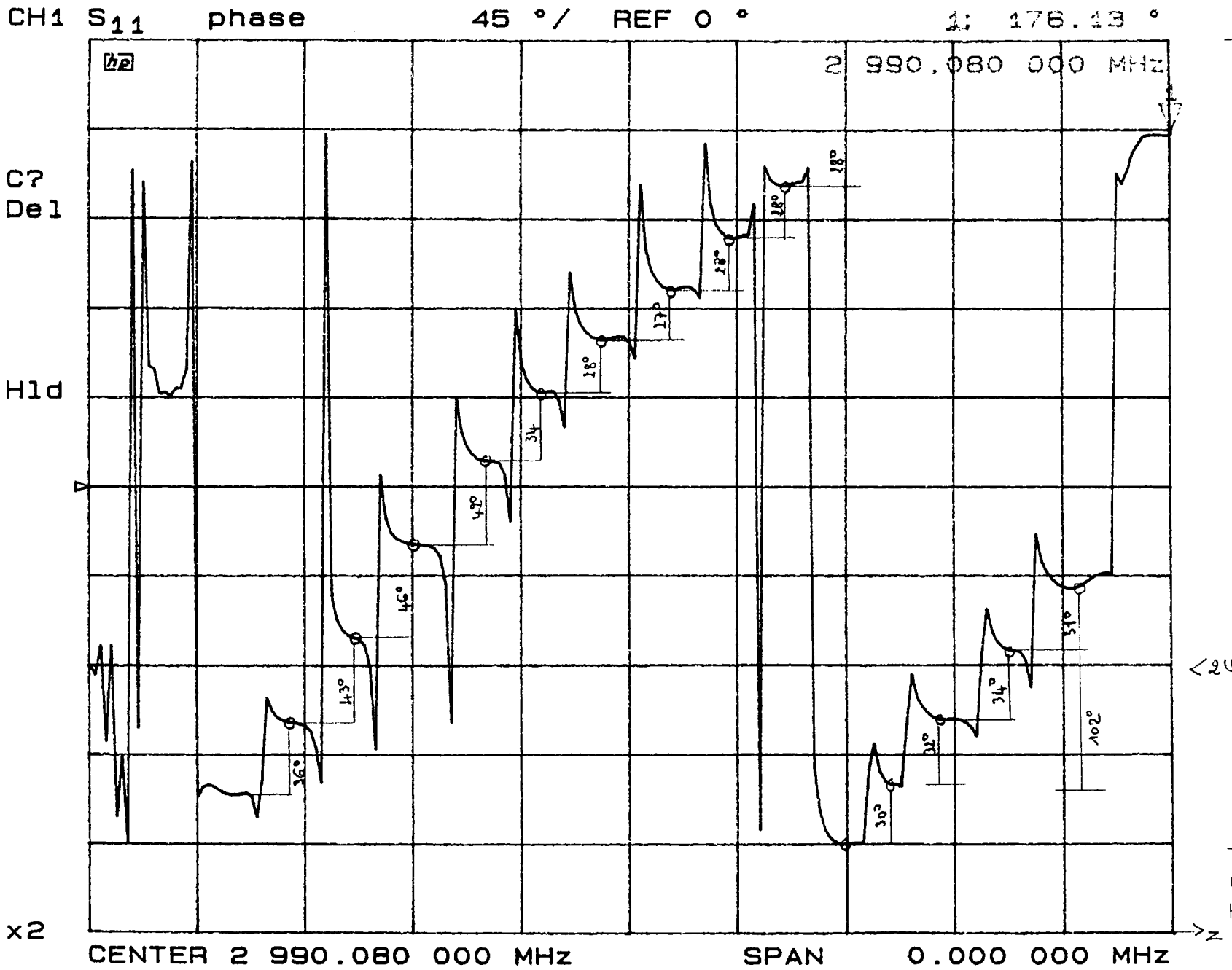

figure 2:

HCS2

2φ [π]

$\langle 2\varphi \rangle = \frac{360+102}{14} = 33{,}0°$

T = 21.4°C
P = 755 T
H = 52%

figure 3:

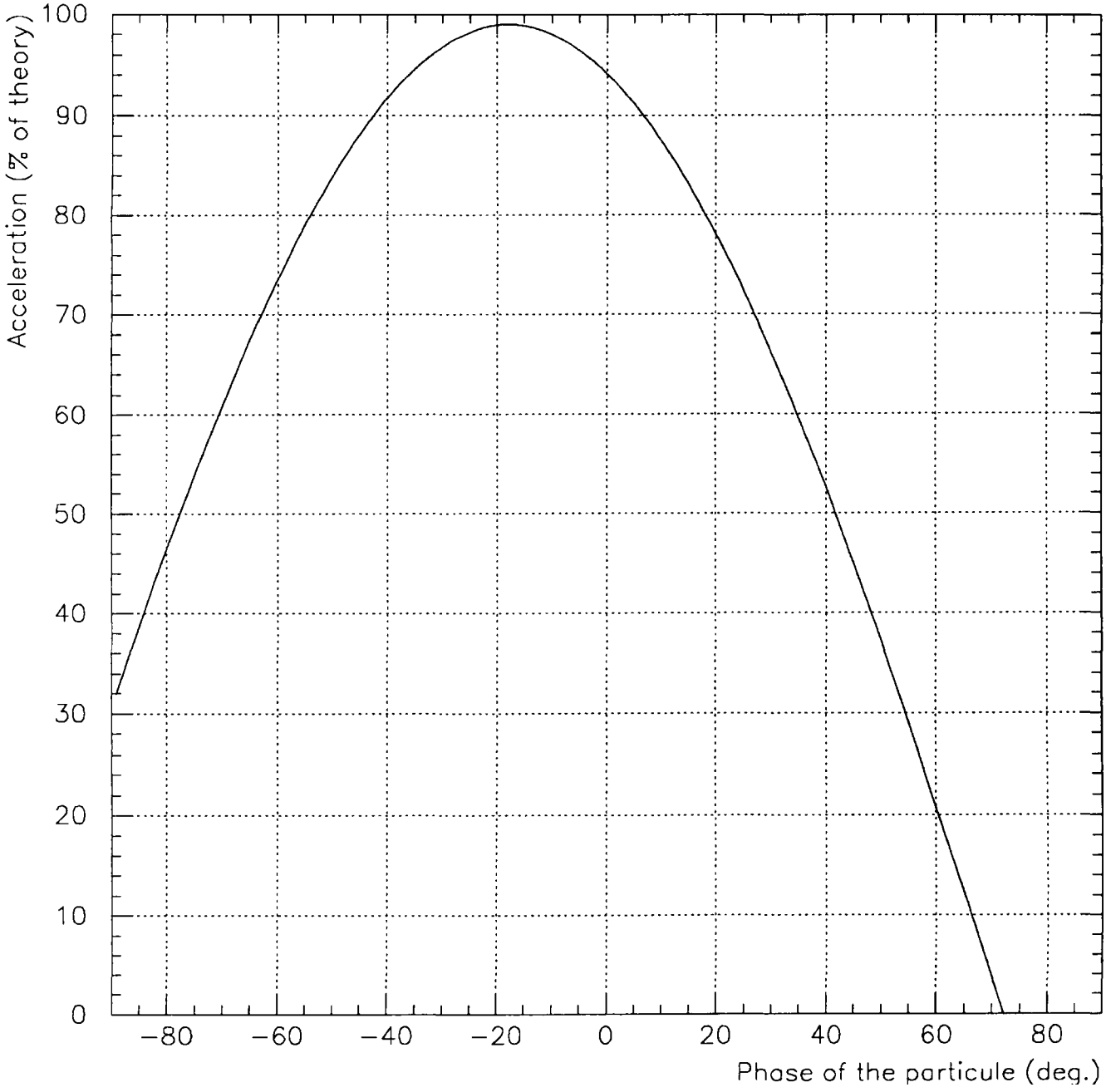
Acceleration (% of theory)
100
90
80
70
60
50
40
30
20
10
0
−80
−60
−40
−20
0
20
40
60
80
Phase of the particule (deg.)

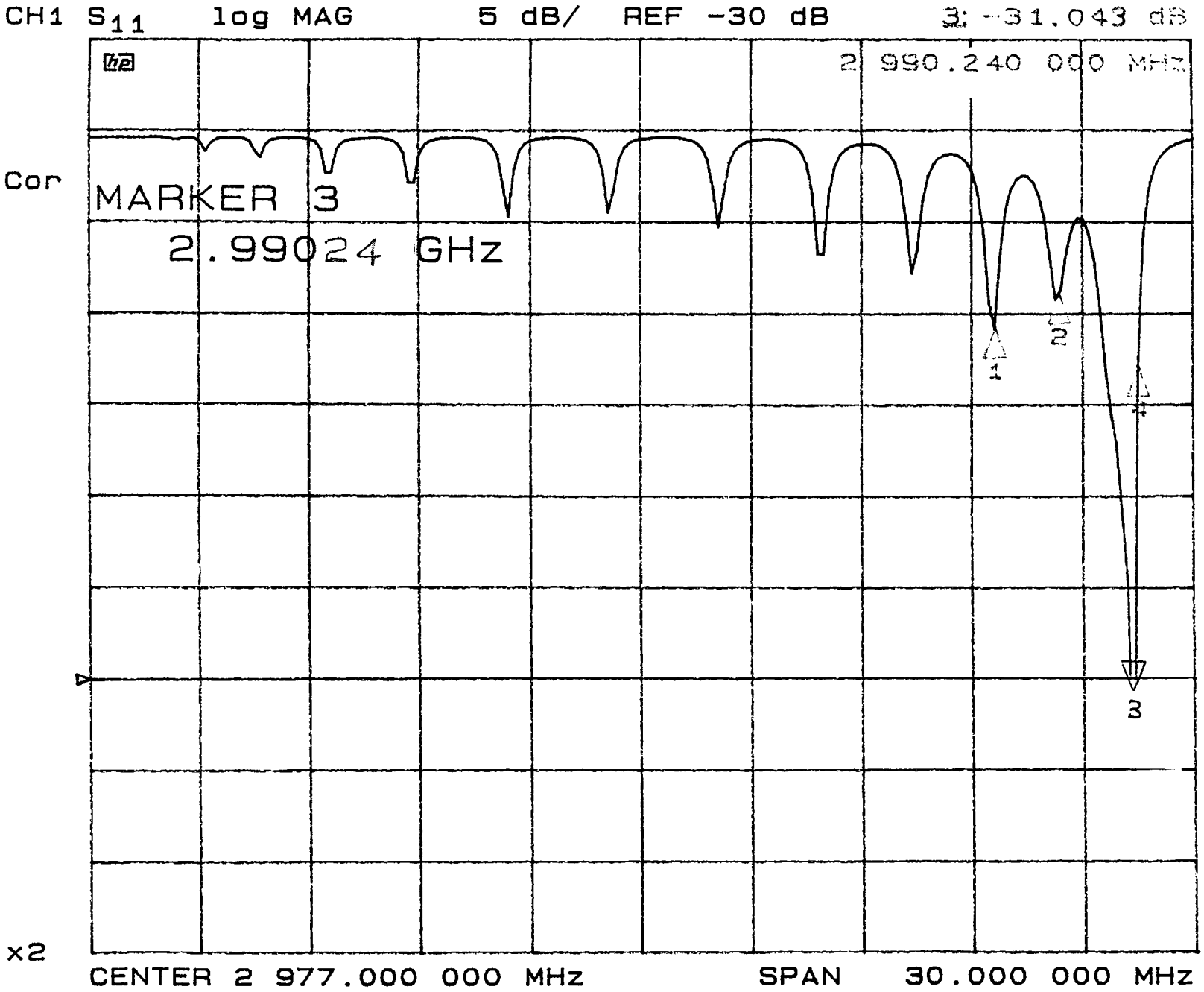

figure 4:

HCS2

$20 \log_{10} r$

1 2986.590 MHz
-10.9 dB

2 2988.550 MHz
-8.9 dB

3. 2990.240 MHz
-31.0 dB

4. 2990.656 MHz
-12.8 dB

T = 19.9°C
P = 755 T
H = 52%

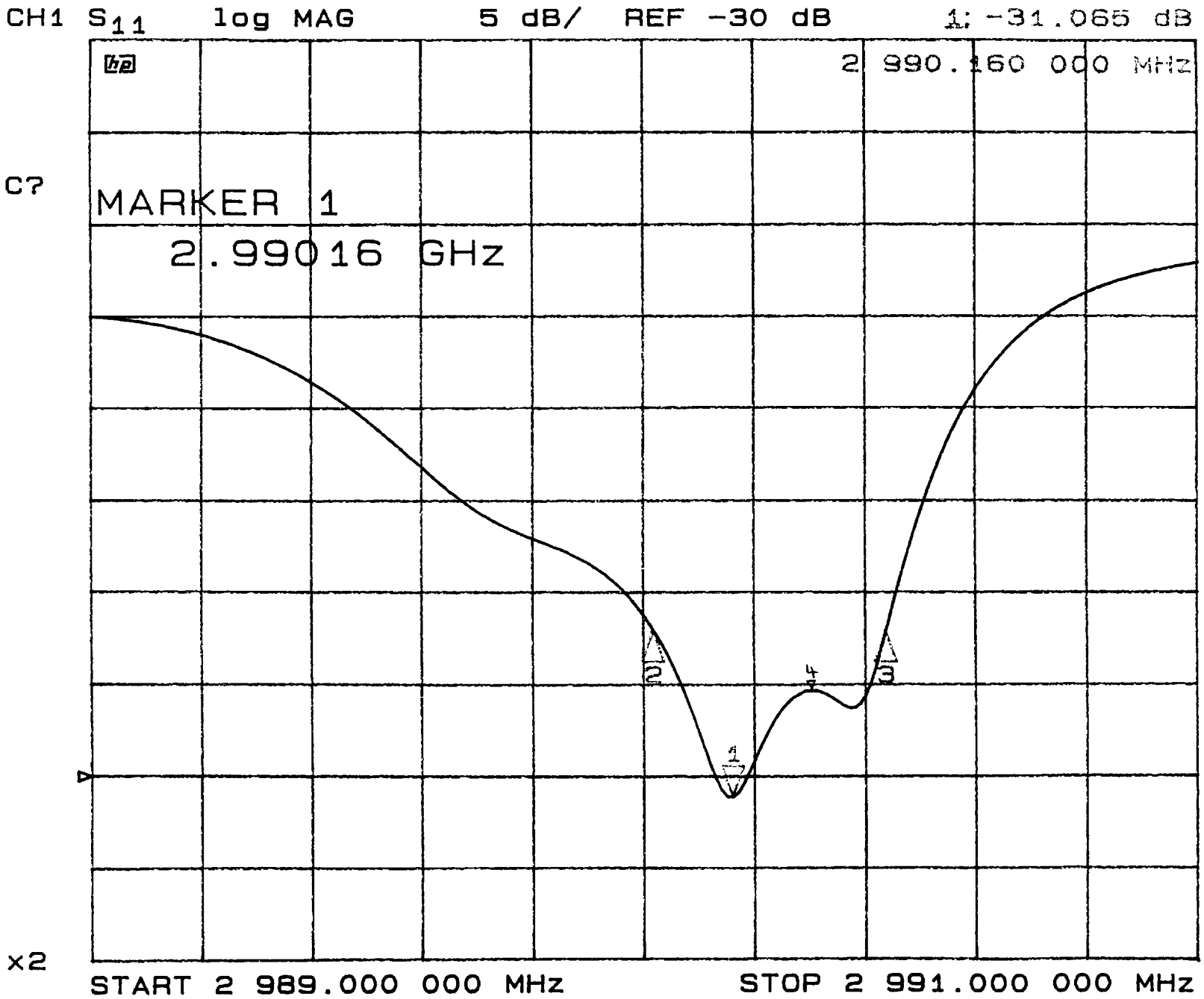

figure 5 :

HCS2

$20 \log_{10} r$

1. 2990.160 MHz
-31.0 dB

2. 2990.017 MHz
-21.9 dB

3. 2990.436 MHz
-22.5 dB

4. 2990.300 MHz
-25.2 dB

T = 19.9°C
P = 755 T
H = 52 %

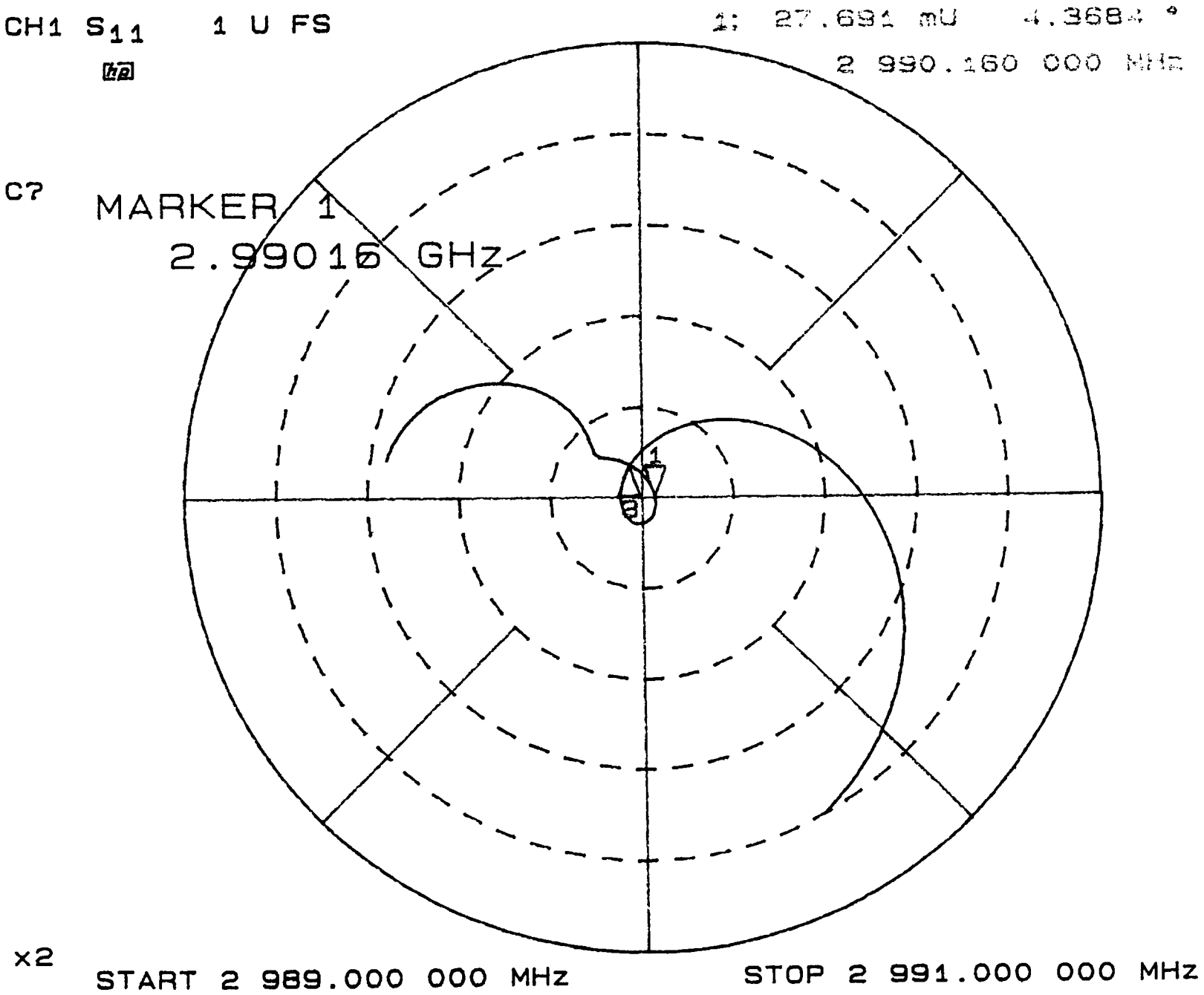

figure 6:

HCS2

Vector n

1. 2990.160 MHz

2. 2990.017 MHz

3. 2990.436 MHz

T = 19.9°C

P = 755 T

H = 52%

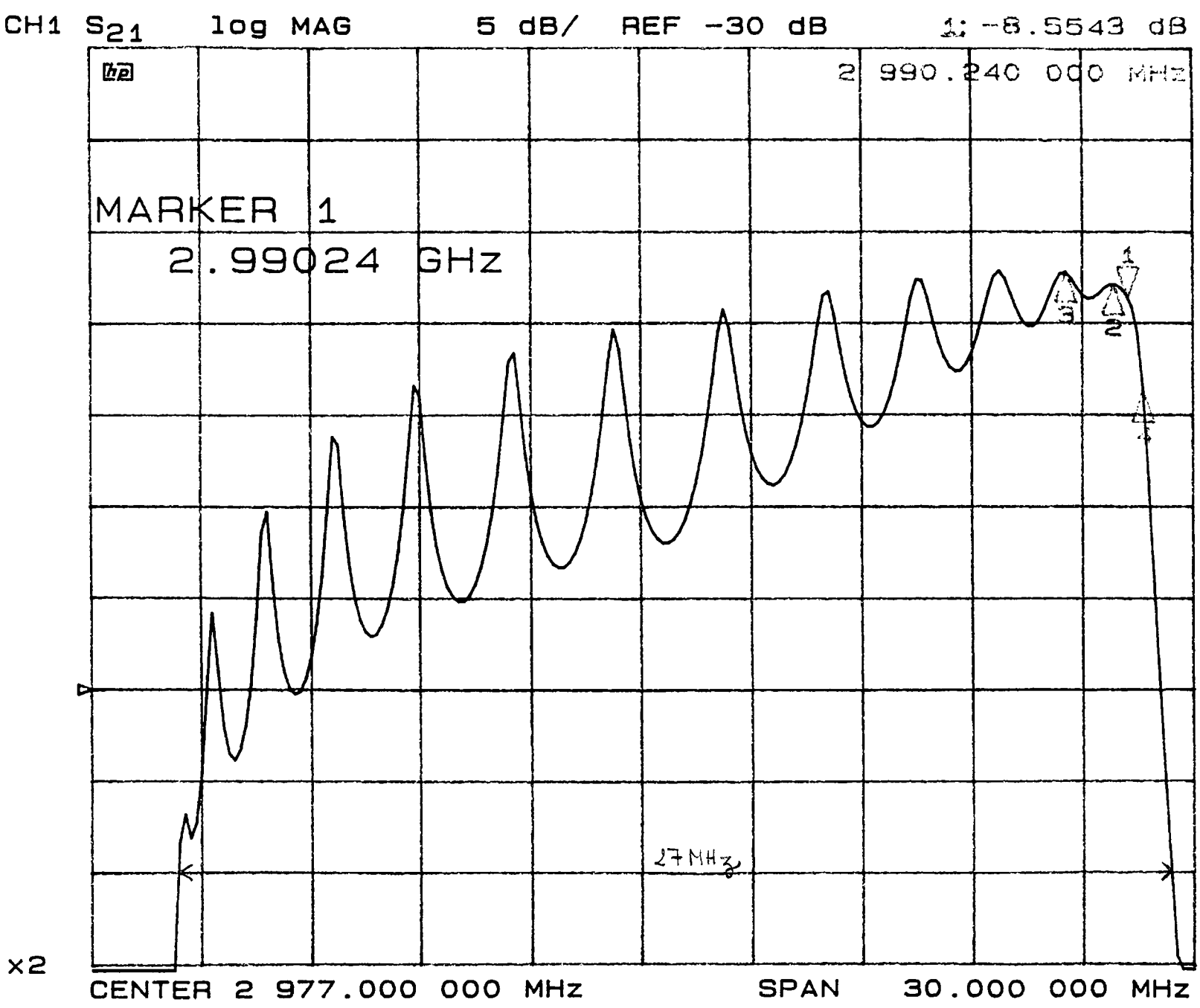

figure 7:

HCS2

$20 \log_{10} t$

Insertion losses:
Hybrid = 3dB
Cables = 1.8dB

1 2990.240 MHz
-8.6dB

2. 2989.840 MHz
-7.8dB

3. 2988.550 MHz
-7.2dB

4 2990.656 MHz
-13.7dB

T = 20.8°C
P = 760 T
H = 48%

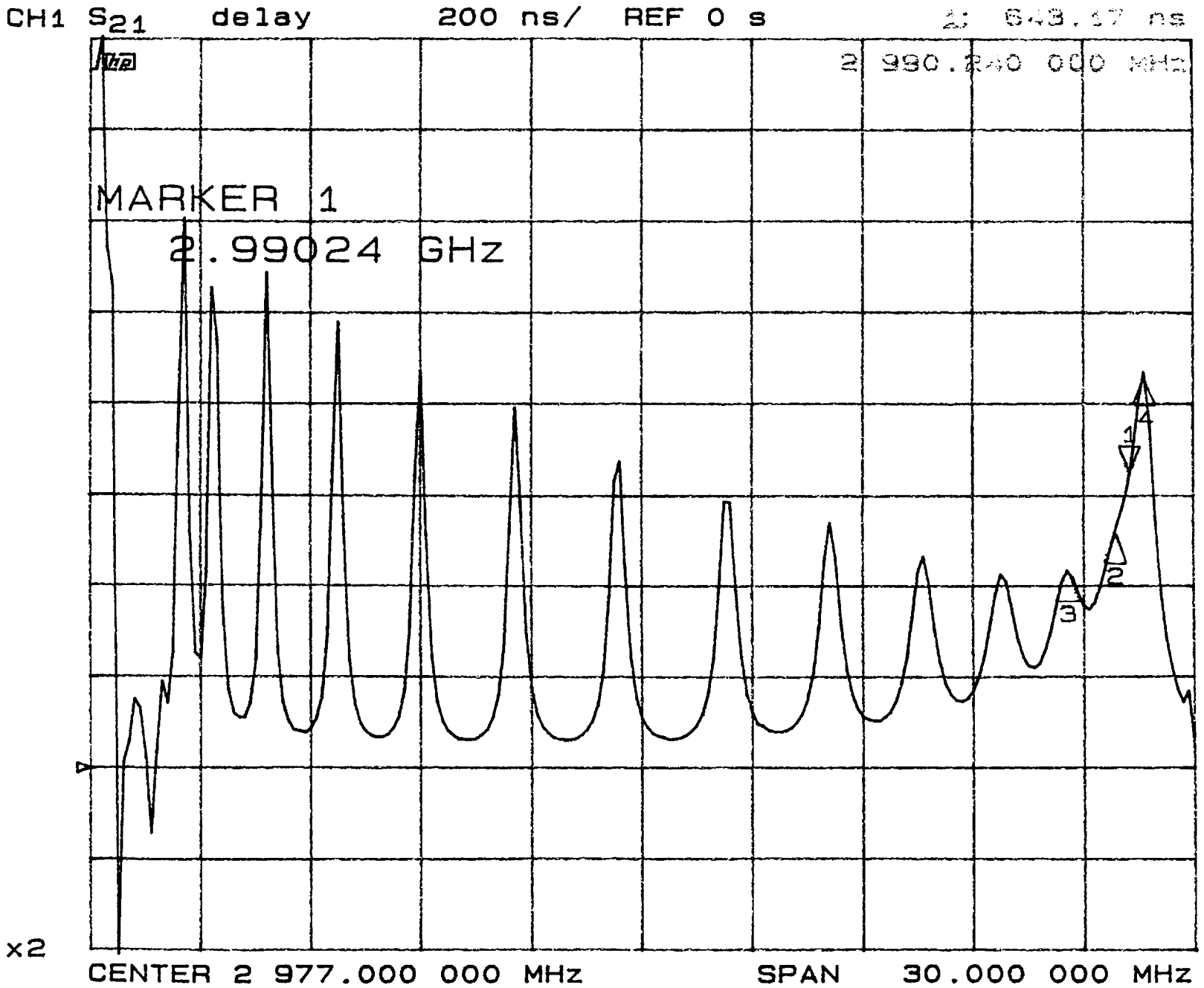

figure 8 :

HCS2

Delay in lout

1. 2990.240 MHz
   643ns

2. 2989.840MHz
   520ns

3. 2988.550MHz
   436ns

4. 2990.656 MHz
   866ns

T = 20.8°C
P = 760 T
H = 48%

figure 9:

HCS2, Measurement of gallagher

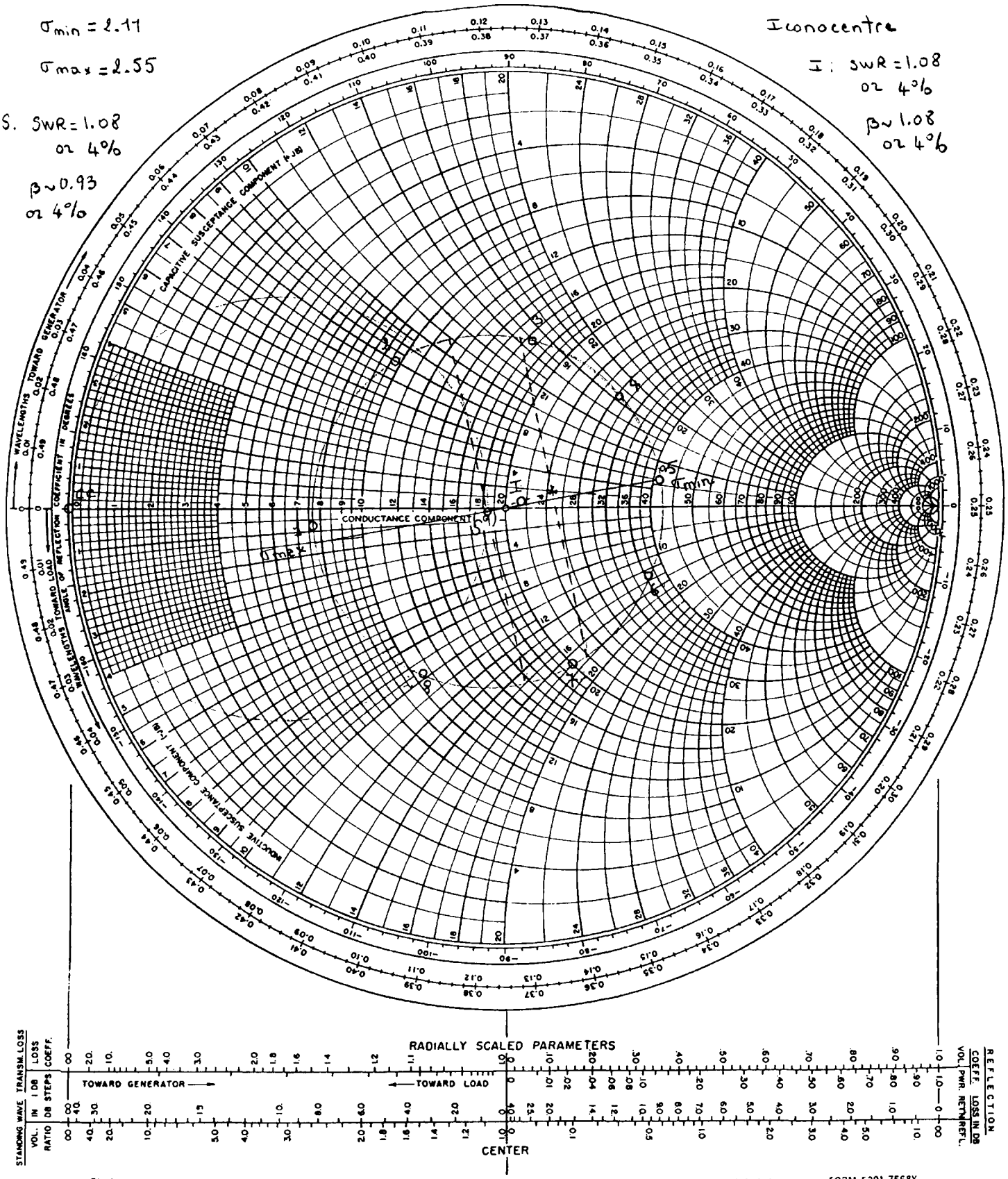

Electronics - VOL 17, NO 1, PP-130-133, 318-325, JAN 1944

GENERAL RADIO COMPANY
WEST CONCORD, MASS.

FORM 5301-7568Y
Printed in USA

Section Attenuation = -4.0dB